PHYSICAL REVIEW D **81,** 052013 (2010)

Measurements of D meson decays to two pseudoscalar mesons

H. Mendez,[1] J. Y. Ge,[2] D. H. Miller,[2] I. P. J. Shipsey,[2] B. Xin,[2] G. S. Adams,[3] D. Hu,[3] B. Moziak,[3] J. Napolitano,[3] K. M. Ecklund,[4] Q. He,[5] J. Insler,[5] H. Muramatsu,[5] C. S. Park,[5] E. H. Thorndike,[5] F. Yang,[5] M. Artuso,[6] S. Blusk,[6] S. Khalil,[6] R. Mountain,[6] K. Randrianarivony,[6] T. Skwarnicki,[6] S. Stone,[6] J. C. Wang,[6] L. M. Zhang,[6] G. Bonvicini,[7] D. Cinabro,[7] A. Lincoln,[7] M. J. Smith,[7] P. Zhou,[7] J. Zhu,[7] P. Naik,[8] J. Rademacker,[8] D. M. Asner,[9] K. W. Edwards,[9] J. Reed,[9] A. N. Robichaud,[9] G. Tatishvili,[9] E. J. White,[9] R. A. Briere,[10] H. Vogel,[10] P. U. E. Onyisi,[11] J. L. Rosner,[11] J. P. Alexander,[12] D. G. Cassel,[12] R. Ehrlich,[12] L. Fields,[12] L. Gibbons,[12] S. W. Gray,[12] D. L. Hartill,[12] B. K. Heltsley,[12] J. M. Hunt,[12] J. Kandaswamy,[12] D. L. Kreinick,[12] V. E. Kuznetsov,[12] J. Ledoux,[12] H. Mahlke-Krüger,[12] J. R. Patterson,[12] D. Peterson,[12] D. Riley,[12] A. Ryd,[12] A. J. Sadoff,[12] X. Shi,[12] S. Stroiney,[12] W. M. Sun,[12] T. Wilksen,[12] J. Yelton,[13] P. Rubin,[14] N. Lowrey,[15] S. Mehrabyan,[15] M. Selen,[15] J. Wiss,[15] M. Kornicer,[16] R. E. Mitchell,[16] M. R. Shepherd,[16] C. M. Tarbert,[16] D. Besson,[17] T. K. Pedlar,[18] J. Xavier,[18] D. Cronin-Hennessy,[19] K. Y. Gao,[19] J. Hietala,[19] T. Klein,[19] R. Poling,[19] P. Zweber,[19] S. Dobbs,[20] Z. Metreveli,[20] K. K. Seth,[20] B. J. Y. Tan,[20] A. Tomaradze,[20] S. Brisbane,[21] J. Libby,[21] L. Martin,[21] A. Powell,[21] C. Thomas,[21] and G. Wilkinson[21]

(CLEO Collaboration)

[1]*University of Puerto Rico, Mayaguez, Puerto Rico 00681*
[2]*Purdue University, West Lafayette, Indiana 47907, USA*
[3]*Rensselaer Polytechnic Institute, Troy, New York 12180, USA*
[4]*Rice University, Houston, Texas 77005, USA*
[5]*University of Rochester, Rochester, New York 14627, USA*
[6]*Syracuse University, Syracuse, New York 13244, USA*
[7]*Wayne State University, Detroit, Michigan 48202, USA*
[8]*University of Bristol, Bristol BS8 1TL, United Kingdom*
[9]*Carleton University, Ottawa, Ontario, Canada K1S 5B6*
[10]*Carnegie Mellon University, Pittsburgh, Pennsylvania 15213, USA*
[11]*University of Chicago, Chicago, Illinois 60637, USA*
[12]*Cornell University, Ithaca, New York 14853, USA*
[13]*University of Florida, Gainesville, Florida 32611, USA*
[14]*George Mason University, Fairfax, Virginia 22030, USA*
[15]*University of Illinois, Urbana-Champaign, Illinois 61801, USA*
[16]*Indiana University, Bloomington, Indiana 47405, USA*
[17]*University of Kansas, Lawrence, Kansas 66045, USA*
[18]*Luther College, Decorah, Iowa 52101, USA*
[19]*University of Minnesota, Minneapolis, Minnesota 55455, USA*
[20]*Northwestern University, Evanston, Illinois 60208, USA*
[21]*University of Oxford, Oxford OX1 3RH, United Kingdom*
(Received 17 June 2009; revised manuscript received 5 March 2010; published 31 March 2010)

Using data collected on the $\psi(3770)$ resonance and near the $D_s^{*\pm}D_s^{\mp}$ peak production energy by the CLEO-c detector, we study the decays of the possible $D \to PP$ modes and report measurements of or upper limits on all branching fractions for Cabibbo-favored, singly Cabibbo-suppressed, and doubly Cabibbo-suppressed $D \to PP$ decays except modes involving K_L^0 (and except $D^0 \to K^+\pi^-$). We normalize with respect to the Cabibbo-favored D modes, $D^0 \to K^-\pi^+$, $D^+ \to K^-\pi^+\pi^+$, and $D_s^+ \to K^+K_S^0$.

DOI: 10.1103/PhysRevD.81.052013 PACS numbers: 13.25.Ft

I. INTRODUCTION

There are many possible exclusive decays of charmed D mesons to a pair of mesons from the lowest-lying pseudoscalar meson nonet. The decay can be to any pair of K^+, K^-, π^+, π^-, η, η', π^0, K^0, or $\bar{K}^0$, with total charge 0 or ± 1. Measurements of the complete set of decays can be used to test flavor topology and SU(3) predictions and to specify strong phases of decay amplitudes through triangle relations [1]. Moreover, many CP asymmetries (expected to be less than $\mathcal{O}(10^{-3})$ in the standard model) can be studied. The detectable neutral kaons are K_S^0 and K_L^0, not K^0 and $\bar{K}^0$, so the observable decays are XK_S^0 and XK_L^0. In this study, we consider only K_S^0, not K_L^0, and report all

 © 2010 The American Physical Society

branching fractions for Cabibbo-favored, singly Cabibbo-suppressed, and doubly Cabibbo-suppressed $D \to PP$ decays except modes involving K_L^0 and except the doubly Cabibbo-suppressed decay $D^0 \to K^+\pi^-$. We normalize with respect to the Cabibbo-favored D modes, $D^0 \to K^-\pi^+$ [2], $D^+ \to K^-\pi^+\pi^+$ [2], and $D_s^+ \to K^+K_S^0$ [3]. (More precisely, we normalize the $D^0 \to PP$ decays with respect to the sum of the Cabibbo-favored mode $D^0 \to K^-\pi^+$ and the doubly Cabibbo-suppressed mode $D^0 \to K^+\pi^-$. The latter is 0.4% of the former.)

II. THE DETECTOR

Data for this analysis were taken at the Cornell Electron Storage Ring (CESR) using the CLEO-c general-purpose solenoidal detector, which is described in detail elsewhere [4–7]. The charged particle tracking system covers a solid angle of 93% of 4π and consists of a small-radius, six-layer, low-mass, stereo wire drift chamber, concentric with, and surrounded by, a 47-layer cylindrical central drift chamber. The chambers operate in a 1.0 T magnetic field. The root-mean-square (rms) momentum resolution achieved with the tracking system is approximately 0.6% at $p = 1$ GeV/c for tracks that traverse all layers of the drift chamber. Photons are detected in an electromagnetic calorimeter consisting of 7800 cesium iodide crystals and covering 95% of 4π, which achieves a photon energy resolution of 2.2% at $E_\gamma = 1$ GeV and 6% at 100 MeV. We utilize two particle identification (PID) devices to separate charged kaons from pions: the central drift chamber, which provides measurements of ionization energy loss (dE/dx), and, surrounding this drift chamber, a cylindrical ring-imaging Cherenkov (RICH) detector, whose active solid angle is 80% of 4π. The combined PID system has a pion or kaon efficiency >85% and a probability of pions faking kaons (or vice versa) <5% [2]. The response of the CLEO-c detector is studied with a detailed GEANT-based [8] Monte Carlo (MC) simulation, with initial particle trajectories generated by EVTGEN [9] and final-state radiation produced by PHOTOS [10]. Simulated events are reconstructed and selected for analysis with the reconstruction programs and selection criteria used for data.

III. THE DATA SAMPLE

For D^0 and D^+ meson decays, we utilize a total integrated luminosity of 818 pb^{-1} of e^+e^- data collected at center-of-mass (c.m.) energies near $E_{\mathrm{c.m.}} = 3774$ MeV. The data sample contains about 2.4×10^6 D^+D^- events (events of interest), 3×10^6 $D^0\bar{D}^0$ events (events of interest), $15 \times 10^6 e^+e^- \to u\bar{u}$, $d\bar{d}$, or $s\bar{s}$ continuum events, 3×10^6 $e^+e^- \to \tau^+\tau^-$ events, and 3×10^6 $e^+e^- \to \gamma\psi'$ radiative return events (sources of background), as well as Bhabha events, μ-pair events, and $\gamma\gamma$ events (useful for luminosity determination and resolution studies). For the D_s^+ meson decays, we use a data sample of $e^+e^- \to D_s^{*\pm}D_s^\mp$ events collected at the c.m. energy 4170 MeV, near $D_s^{*\pm}D_s^\mp$ peak production of ~1 nb [11]. The data sample consists of an integrated luminosity of 586 pb^{-1} containing about 5.4×10^5 $D_s^{*\pm}D_s^\mp$ pairs. Other charm production totals ~7 nb [11], and the underlying light-quark "continuum" is about 12 nb. Through this paper, charge conjugate modes are implicitly assumed, unless otherwise noted.

IV. PROCEDURE

A. D^0 and D^+

Here we employ a single-tag technique extensively used by CLEO-c [2,3,12,13], pioneered by the Mark III Collaboration at SPEAR for measuring D^0 and D^+ branching fractions [14,15], which exploits a feature of near-threshold production of charmed mesons, i.e. M_{bc} and ΔE, see below.

We formed D and $\bar{D}$ candidates in all $D \to PP$ decay modes from combinations of $\pi^\pm$, $K^\pm$, π^0, K_S^0, η, and η' candidates selected using the standardized requirements which are common to many CLEO-c analyses involving D decays. The $\psi(3770)$ resonance is below the kinematic threshold for $D\bar{D}\pi$ production, so the events of interest, $e^+e^- \to \psi(3770) \to D\bar{D}$, have D mesons with energy equal to the beam energy. Two variables reflecting energy and momentum conservation are used to identify valid D candidates. They are $\Delta E \equiv \sum_i E_i - E_{\mathrm{beam}}$, and

$$M_{\mathrm{bc}} \equiv \sqrt{E_{\mathrm{beam}}^2 - \left(\sum_i \mathbf{p}_i\right)^2},$$

where E_i, $\mathbf{p}_i$ are the energy and momentum of the decay products of a D candidate. For a correct combination of particles, ΔE will be consistent with zero, and the beam-constrained mass M_{bc} will be consistent with the D mass. Candidates are rejected if they fail mode-dependent ΔE requirements. If there is more than one candidate in a particular D or $\bar{D}$ decay mode, we choose the candidate with the smallest $|\Delta E|$.

B. D_s^+

Unlike $D\bar{D}$ threshold events, conventional ΔE and M_{bc} variables are no longer good variables for D_s from $D_s^{*+}D_s^-$ decays, as the D_s can either be a primary or secondary (from a D_s^* decay), with different momentum. We use the reconstructed invariant mass of the D_s candidate, $M(D_s)$, and the mass recoiling against the D_s candidate, $M_{\mathrm{recoil}}(D_s) \equiv \sqrt{(E_0 - E_{D_s})^2 - (\mathbf{p}_0 - \mathbf{p}_{D_s})^2}$, as our primary kinematic variables to select a D_s candidate. Here $(E_0, \mathbf{p}_0)$ is the net four-momentum of the e^+e^- system, taking the finite beam crossing angle into account, $\mathbf{p}_{D_s}$ is the momentum of the D_s candidate, $E_{D_s} = \sqrt{m_{D_s}^2 + \mathbf{p}_{D_s}^2}$, and m_{D_s} is the known D_s mass [16]. We make no requirements on the decay of the other D_s in the event.

There are two components in the recoil mass distribution, a peak around the D_s^* mass if the candidate is due to the primary D_s and a rectangular shaped distribution if the candidate is due to the secondary D_s from a D_s^* decay. The edges of $M_{\rm recoil}(D_s)$ from the secondary D_s are kinematically determined (as a function of $\sqrt{s}$ and known masses), and at $\sqrt{s} = 4170$ MeV, $\Delta M_{\rm recoil}(D_s) \equiv M_{\rm recoil}(D_s) - m_{D_s^*}$ is in the range $[-54, 57]$ MeV. Initial state radiation causes a tail on the high side, above 57 MeV. We select D_s candidates within the $-55\ {\rm MeV} \leq \Delta M_{\rm recoil}(D_s) < +55$ MeV range. This window allows both primary and secondary D_s candidates to be selected.

We also require a photon consistent with coming from $D_s^{*+} \to D_s^+ \gamma$ decay, by looking at the mass recoiling against the D_s candidate plus γ system, $M_{\rm recoil}(D_s\gamma) \equiv \sqrt{(E_0 - E_{D_s} - E_\gamma)^2 - (\mathbf{p}_0 - \mathbf{p}_{D_s} - \mathbf{p}_\gamma)^2}$. For correct combinations, this recoil mass peaks at m_{D_s}, regardless of whether the candidate is due to a primary or a secondary D_s. We require $|M_{\rm recoil}(D_s\gamma) - m_{D_s}| < 30$ MeV. This requirement improves the signal to noise ratio, important for the suppressed modes. Every event is allowed to contribute a maximum of one D_s candidate per mode and charge. If there are multiple candidates, the one with $M_{\rm recoil}(D_s\gamma)$ closest to m_{D_s} is chosen.

C. Common

Our standard final-state particle selection requirements are described in detail elsewhere [2]. Charged tracks produced in the D decay are required to satisfy criteria based on the track fit quality, and angles θ with respect to the beam line, satisfying $|\cos\theta| < 0.93$. Momenta of charged particles utilized in D^0 and D^+ candidate reconstructions must be above 50 MeV/c, while those for D_s must be above 100 MeV/c to eliminate the soft pions from $D^*\bar{D}^*$ and $D^*\bar{D}$ decays (through $D^* \to \pi D$). Tracks must also be consistent with their coming from the interaction point in three dimensions. Pion and kaon candidates are required to have dE/dx measurements within 3 standard deviations (3σ) of the expected value. For tracks with momenta greater than 700 MeV/c, RICH information, if available, is combined with dE/dx.

The K_S^0 candidates are selected from pairs of oppositely charged and vertex-constrained tracks having invariant mass within 7.5 MeV, or roughly 3σ, of the known K_S^0 mass [16]. We identify π^0 candidates via $\pi^0 \to \gamma\gamma$, de-

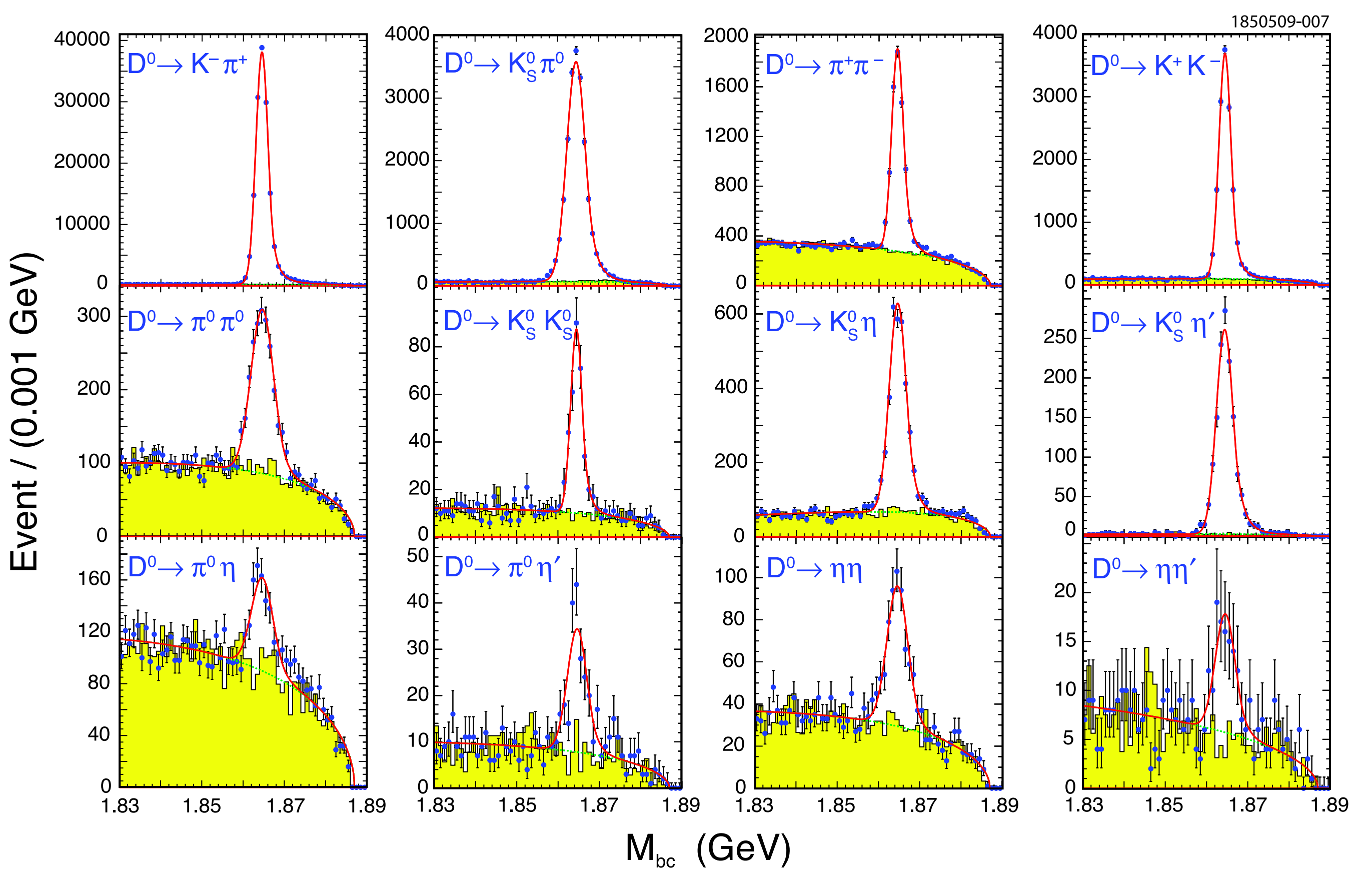

FIG. 1 (color online). $M_{\rm bc}$ distributions of D^0 modes. For each distribution, the points are obtained from the ΔE signal region, the shaded histogram is from the ΔE sidebands, and the line is the fit.

tecting the photons in the CsI calorimeter. To avoid having both photons in a region of poorer energy resolution, we require that at least one of the photons be in the "good barrel" region, $|\cos\theta_\gamma| < 0.80$. We require that a calorimeter cluster has a measured energy above 30 MeV, has a lateral distribution consistent with that from photons, and not be matched to any charged track. The invariant mass of the photon pair is required to be within 3σ ($\sigma \sim 6$ MeV) of the known π^0 mass. A π^0 mass constraint is imposed when π^0 candidates are used in further reconstruction. We reconstruct η candidates in the decay of $\eta \to \gamma\gamma$. Candidates are formed using a similar procedure as for π^0 except that $\sigma \sim 12$ MeV. We reconstruct η' candidates in the decay mode $\eta' \to \pi^+\pi^-\eta$. We require $|m_{\pi^+\pi^-\eta} - m_{\eta'}| < 10$ MeV.

V. RESULTS

A. D^0 and D^+

The M_{bc} distributions for the D^0 and D^+ candidate combinations are shown in Figs. 1 and 2, respectively. The points show the data and the lines are fits. The normalization modes $D^0 \to K^-\pi^+$ and $D^+ \to K^-\pi^+\pi^+$ are essentially background free. The backgrounds of all modes are well described by the distributions obtained from the ΔE sidebands. We perform a binned maximum likelihood fit to extract the D^0 or D^+ signal yield from each M_{bc} distribution. For the signal, we use an inverted Crystal Ball line shape [17], which is a Gaussian with a high-side tail. For high-statistics modes ($D^0 \to K^+K^-$, $K^-\pi^+$, $K^0_S\pi^0$, $K^0_S\eta'$, and $D^+ \to K^-\pi^+\pi^+$, $K^0_SK^+$, $K^0_S\pi^+$), we leave all Crystal Ball parameters free, determining them in the fit. For other D^0 and D^+ modes (lower statistics modes), Crystal Ball parameters were taken from fits to Monte Carlo events. Monte Carlo accuracy was checked in studies with the high-statistics modes, and found to be in good agreement with the parameters found in fits to the data. For the background, we use an ARGUS function [18], with the shape parameter determined from the ΔE sideband M_{bc} distribution, the high-end cutoff given by E_{beam}, and the normalization determined from the fit to the ΔE signal region. We verified the correctness of this procedure with Monte Carlo simulation. The ΔE signal and sideband regions are mode dependent, and of comparable width. Results of the fits are shown in Table I. Table I also includes the detection efficiency for each mode. The effi-

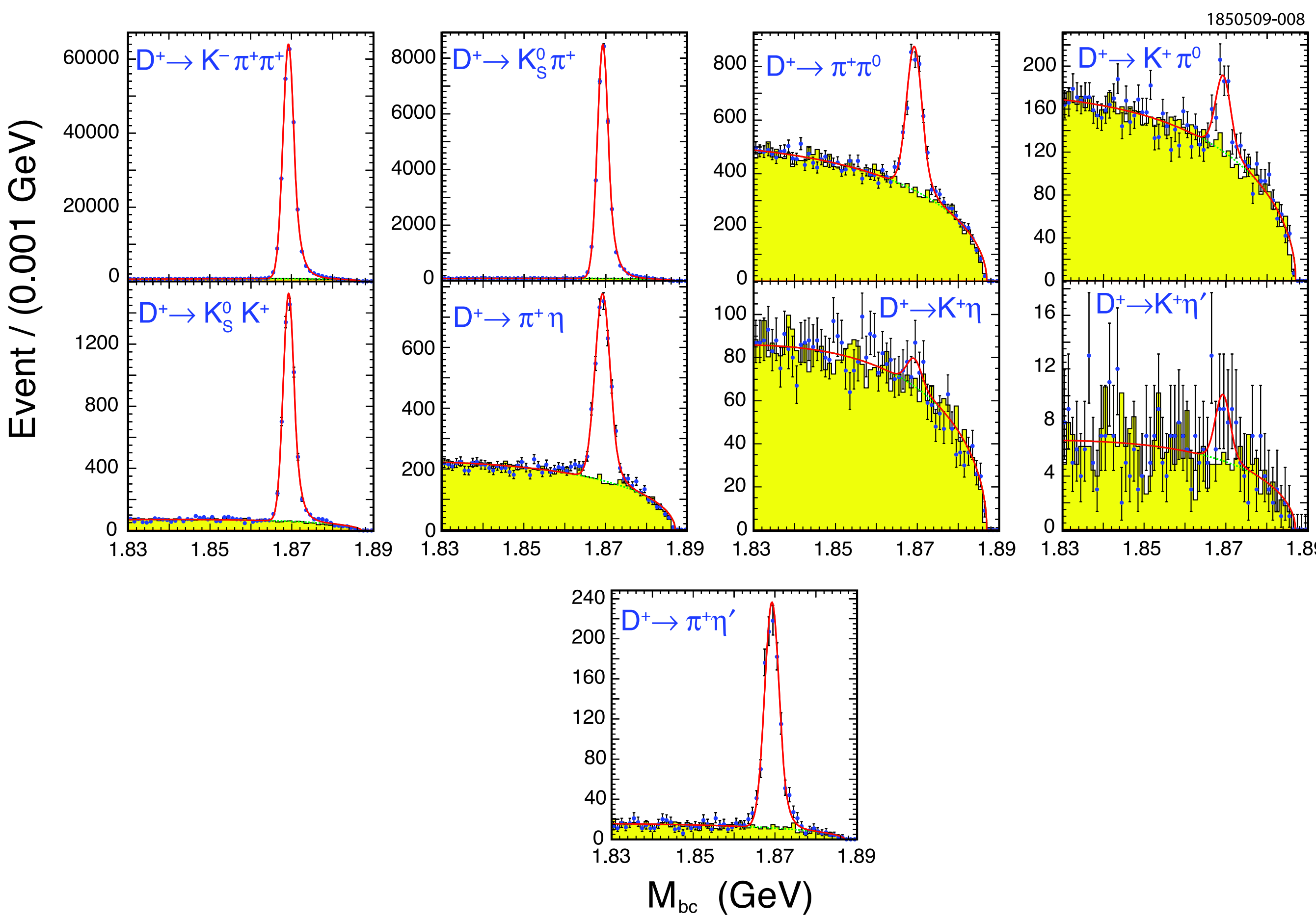

FIG. 2 (color online). M_{bc} distributions of D^+ modes. For each distribution, the points are obtained from the ΔE signal region, the shaded histogram is from the ΔE sidebands, and the line is the fit.

TABLE I. Observed yields from data and reconstruction efficiencies and their statistical uncertainties. The efficiencies include submode branching fractions [16] and have been corrected to include several known small differences between data and Monte Carlo simulation.

Mode	Efficiency (%)	Yield
$D^0 \to K^+K^-$	57.35 ± 0.16	13782 ± 136
$D^0 \to K_S^0 K_S^0$	22.73 ± 0.13	215 ± 23
$D^0 \to \pi^+\pi^-$	72.68 ± 0.14	6210 ± 93
$D^0 \to \pi^0\pi^0$	32.95 ± 0.14	1567 ± 54
$D^0 \to K^-\pi^+$	65.11 ± 0.15	150259 ± 420
$D^0 \to K_S^0\pi^0$	28.57 ± 0.14	20045 ± 165
$D^0 \to K_S^0\eta$	10.08 ± 0.05	2864 ± 65
$D^0 \to \pi^0\eta$	11.97 ± 0.05	481 ± 40
$D^0 \to K_S^0\eta'$	2.35 ± 0.02	1321 ± 42
$D^0 \to \pi^0\eta'$	2.97 ± 0.02	159 ± 19
$D^0 \to \eta\eta$	4.35 ± 0.02	430 ± 29
$D^0 \to \eta\eta'$	1.06 ± 0.01	66 ± 15
$D^+ \to K^-\pi^+\pi^+$	54.92 ± 0.16	231058 ± 515
$D^+ \to K_S^0 K^+$	36.62 ± 0.15	5161 ± 86
$D^+ \to \pi^+\pi^0$	48.69 ± 0.15	2649 ± 76
$D^+ \to K_S^0\pi^+$	42.54 ± 0.16	30095 ± 191
$D^+ \to K^+\pi^0$	43.29 ± 0.15	343 ± 37
$D^+ \to K^+\eta$	15.95 ± 0.06	60 ± 24
$D^+ \to \pi^+\eta$	18.07 ± 0.06	2940 ± 68
$D^+ \to K^+\eta'$	4.29 ± 0.02	23 ± 18
$D^+ \to \pi^+\eta'$	4.81 ± 0.02	1037 ± 35
$D_s^+ \to K_S^0 K^+$	24.73 ± 0.14	4076 ± 71
$D_s^+ \to \pi^+\pi^0$	16.60 ± 0.12	19 ± 28
$D_s^+ \to K_S^0\pi^+$	28.15 ± 0.14	393 ± 33
$D_s^+ \to K^+\pi^0$	29.57 ± 0.14	202 ± 70
$D_s^+ \to K^+\eta$	11.40 ± 0.05	222 ± 41
$D_s^+ \to \pi^+\eta$	12.70 ± 0.06	2587 ± 89
$D_s^+ \to K^+\eta'$	2.87 ± 0.02	56 ± 17
$D_s^+ \to \pi^+\eta'$	3.28 ± 0.02	1436 ± 47

ciencies include submode branching fractions [16] and have been corrected to include four known small differences between data and Monte Carlo simulation, in particular π^0-finding efficiency 0.96, η-finding efficiency 0.935, $\pi^\pm$ particle identification 0.995, and $K^\pm$ particle identification 0.99, data efficiency being smaller than MC efficiency by those ratios.

B. D_s^+

The resulting $M(D_s)$ distributions for D_s modes are shown in Fig. 3. The points show the data and the lines are fits. We perform binned maximum likelihood fits to extract signal yields from the $M(D_s)$ distributions. For the signal, we use the sum of two Gaussians for the line shape. We fix the parameters of two Gaussians to the Monte Carlo simulation. We repeat the fit with all parameters free and take the difference as the systematic uncertainty. For the background, we use a second-degree polynomial function. We float all of the background shape parameters during the fit. Results of the fits and detection efficiencies are given in Table I.

C. Upper limits

For most of the $D \to PP$ modes, very clear signals are found in data. We find no significant evidence for $D^+ \to K^+\eta$, $D^+ \to K^+\eta'$, and $D_s^+ \to \pi^+\pi^0$ decays, and therefore set upper limits on their branching fractions. The $M_{\rm bc}$ distributions of $D^+ \to K^+\eta$ and $D^+ \to K^+\eta'$ modes are shown in Fig. 2. Monte Carlo studies indicate that tightening the requirements on $M_{\rm recoil}(D_s)$ to ± 10 MeV and $M_{\rm recoil}(D_s\gamma)$ to ± 20 MeV should improve the upper limit on $D_s^+ \to \pi^+\pi^0$ decay. Consequently, for $D_s^+ \to \pi^+\pi^0$ (and only $D_s^+ \to \pi^+\pi^0$), we have applied these tighter requirements. The invariant mass distribution for $D_s^+ \to \pi^+\pi^0$ shown in Fig. 3 and the efficiency given in Table I have these tighter requirements.

D. Background from nonresonant decays

Nonresonant D decays can enter into our signal modes with the same final particles. For example, nonresonant $D^+ \to \pi^+(\pi^+\pi^-)$ can appear in the $D^+ \to \pi^+ K_S^0$, $K_S^0 \to \pi^+\pi^-$ mode. Also, nonresonant $D^+ \to \pi^+(\pi^+\pi^-\eta)$ can appear in the $D^+ \to \pi^+\eta'$, $\eta' \to \pi^+\pi^-\eta$ mode. To understand the backgrounds from nonresonant D^0 or D^+ decays, we look at $M_{\rm bc}$ distributions in the invariant mass sideband regions of the intermediate resonances (K_S^0 or η'). For D_s^+ decays, we follow the same procedure, replacing $M_{\rm bc}$ with $M(D_s)$. The scaling factor, from sideband to signal region, is taken to be unity, as indicated by Monte Carlo studies.

For the $D^0 \to K_S^0 K_S^0$ (or $D^0 \to K_S^0\eta'$) mode, the scatter plot of K_S^0 candidate invariant mass against the other K_S^0 (or η') candidate invariant mass is used to define a signal region and two kinds of sideband regions to remove the nonresonant decay background. Again, the scaling factor, from sideband to signal region, is taken to be unity.

Peaking background from particle misidentification (e.g., $D^0 \to K^-\pi^+$, with K^- misidentified as π^-, as background to $D^0 \to \pi^+\pi^-$) fails the ΔE cut, and so is not a problem. Cross feed among $D^0 \to \pi^0\pi^0$, $\pi^0\eta$, and $\eta\eta$ was studied in Monte Carlo simulation, and found to be negligible. Monte Carlo studies found no sources of backgrounds that peaked in the signal region, other than the background from nonresonant decays, discussed above.

E. Systematic uncertainties

We have considered several sources of systematic uncertainty. Some are correlated among different decay modes. These include:

(1) the uncertainty associated with the efficiency for finding a track—0.3% per track [2];
(2) an additional 0.6% per kaon track is added [2], uncorrelated with item 1;

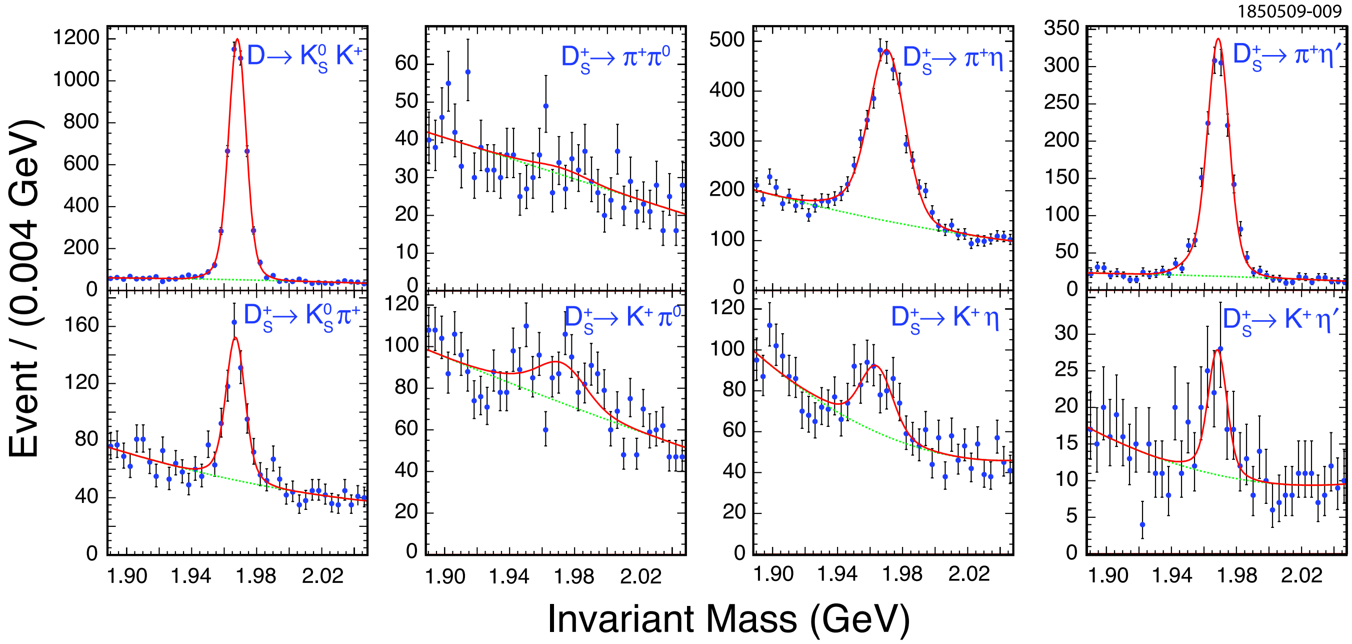

FIG. 3 (color online). $M(D_s)$ distributions for D_s modes. For each distribution, the points are the data and the superimposed line is the fit (the dotted line is the fitted background). The distribution for $D_s^+ \to \pi^+\pi^0$ has tighter requirements than the other modes—see text.

(3) the uncertainty in charged pion identification is 0.3% per $\pi^\pm$ [2];
(4) the uncertainty in charged kaon identification is 0.3% per $K^\pm$ [2], uncorrelated with item 3;
(5) the relative systematic uncertainties for π^0, K_S^0, and η finding efficiencies are 2.0%, 1.8% [2], and 4.0% [3], independent of one another, and independent of the first four-mentioned uncertainties;
(6) finally, among the correlated systematic uncertainties, there are the uncertainties in the input branching fractions of the normalization modes, 2.0% for $D^0 \to K^-\pi^+$ [2], 2.2% for $D^+ \to K^-\pi^+\pi^+$ [2], and 5.8% for $D_s^+ \to K_S^0K^+$ [3].

Note that for K_S^0, with $K_S^0 \to \pi^+\pi^-$, item 1 applies, as the tracks must be found, but item 3 does not apply, as pion identification is not required for $K_S^0 \to \pi^+\pi^-$.

To illustrate the first four sources, consider $D^0 \to K^+K^-$ and $D^0 \to \pi^+\pi^-$, measured relative to our reference mode $D^0 \to K^-\pi^+$. There is no contribution from item 1, as all three modes have the same number of tracks. From item 2, there is a 0.6% to both decay modes, but of opposite sign, as one has one more kaon, and the other has one fewer kaon, than the reference mode. From items 3 and 4, there is a 0.3% contribution from each, because of one more, or one fewer, pion, and ditto from one more, or one fewer kaon.

The systematic uncertainties that are uncorrelated among the decay modes include those due to choice of signal shape and background shape. For the decay modes whose signal shape parameters were not left as free parameters, but taken from Monte Carlo studies, we determine a systematic error by making reasonable variations in those parameters, based on the comparisons of data and Monte Carlo events for high-statistics modes. They range from $\pm 0.77\%$ for the cleaner decay modes to $\pm 4.55\%$ for the modes with substantial background.

We studied the systematic error from the choice of bin size in our binned maximum likelihood fits, by repeating the fits using bins half as wide, and taking the change as the systematic error from that source. The changes varied from 0.003% to 4.1%, the larger values occurring for very low statistics modes.

In Table II we separately list, for each decay mode, the quadratic sum of the systematic errors excluding that from the normalization mode, and the error from the uncertainty in the normalization mode.

F. *CP* asymmetries

The standard model predicts that direct *CP* violation in D decays, e.g., a difference in the branching fractions for $D_s^+ \to K^+\eta$ and $D_s^- \to K^-\eta$, will be vanishingly small. We have separate yields and efficiencies for D and $\bar{D}$ events, so it is possible to compute asymmetries $\mathcal{A}_{CP} \equiv (\mathcal{B}_+ - \mathcal{B}_-)/(\mathcal{B}_+ + \mathcal{B}_-)$, which are sensitive to direct *CP* violation in D decays. All systematic uncertainties cancel in this ratio, with the exception of charged pion and kaon tracking and particle identification efficiencies. Here the relative factor is the charge dependence of the efficiencies in data and Monte Carlo simulations [2]. The charge

TABLE II. Ratios of branching fractions to the corresponding normalization modes $D^0 \to K^-\pi^+$, $D^+ \to K^-\pi^+\pi^+$, and $D_s^+ \to K_S^0 K^+$; branching fraction results from this analysis; and charge asymmetries $\mathcal{A}_{CP}$. Uncertainties are statistical error, systematic error, and the error from the input branching fractions of normalization modes. In the column labeled Previous, S with a citation indicates that this result supersedes the previous result; A with a citation indicates that this result is statistically independent of the previous measurement and can be averaged with it assuming that the systematic errors are fully correlated; N without a citation indicates that there is no previous CLEO-c measurement; and I with a citation indicates that this is an external input normalization branching fraction. Note that the D^0 normalization mode is the sum of $D^0 \to K^-\pi^+$ and $D^0 \to K^+\pi^-$ (see text).

Mode	$\mathcal{B}_{\rm mode}/\mathcal{B}_{\rm Normalization}$ (%)	This result $\mathcal{B}$ (%)	$\mathcal{A}_{CP}$ (%)	Previous
$D^0 \to K^+K^-$	$10.41 \pm 0.11 \pm 0.12$	$0.407 \pm 0.004 \pm 0.005 \pm 0.008$		S [19]
$D^0 \to K_S^0 K_S^0$	$0.41 \pm 0.04 \pm 0.02$	$0.0160 \pm 0.0017 \pm 0.0008 \pm 0.0003$		S [19]
$D^0 \to \pi^+\pi^-$	$3.70 \pm 0.06 \pm 0.09$	$0.145 \pm 0.002 \pm 0.004 \pm 0.003$		S [20]
$D^0 \to \pi^0\pi^0$	$2.06 \pm 0.07 \pm 0.10$	$0.081 \pm 0.003 \pm 0.004 \pm 0.002$		S [20]
$D^0 \to K^-\pi^+$	100	3.9058 external input	$0.5 \pm 0.4 \pm 0.9$	I [2]
$D^0 \to K_S^0\pi^0$	$30.4 \pm 0.3 \pm 0.9$	$1.19 \pm 0.01 \pm 0.04 \pm 0.02$		S [21]
$D^0 \to K_S^0\eta$	$12.3 \pm 0.3 \pm 0.7$	$0.481 \pm 0.011 \pm 0.026 \pm 0.010$		S [22]
$D^0 \to \pi^0\eta$	$1.74 \pm 0.15 \pm 0.11$	$0.068 \pm 0.006 \pm 0.004 \pm 0.001$		A [20] S [23]
$D^0 \to K_S^0\eta'$	$24.3 \pm 0.8 \pm 1.1$	$0.95 \pm 0.03 \pm 0.04 \pm 0.02$		N
$D^0 \to \pi^0\eta'$	$2.3 \pm 0.3 \pm 0.2$	$0.091 \pm 0.011 \pm 0.006 \pm 0.002$		S [23]
$D^0 \to \eta\eta$	$4.3 \pm 0.3 \pm 0.4$	$0.167 \pm 0.011 \pm 0.014 \pm 0.003$		S [23]
$D^0 \to \eta\eta'$	$2.7 \pm 0.6 \pm 0.3$	$0.105 \pm 0.024 \pm 0.010 \pm 0.002$		S [23]
$D^+ \to K^-\pi^+\pi^+$	100	9.1400 external input	$-0.1 \pm 0.4 \pm 0.9$	I [2]
$D^+ \to K_S^0 K^+$	$3.35 \pm 0.06 \pm 0.07$	$0.306 \pm 0.005 \pm 0.007 \pm 0.007$	$-0.2 \pm 1.5 \pm 0.9$	S [19]
$D^+ \to \pi^+\pi^0$	$1.29 \pm 0.04 \pm 0.05$	$0.118 \pm 0.003 \pm 0.005 \pm 0.003$	$2.9 \pm 2.9 \pm 0.3$	S [20]
$D^+ \to K_S^0\pi^+$	$16.82 \pm 0.12 \pm 0.37$	$1.537 \pm 0.011 \pm 0.034 \pm 0.033$	$-1.3 \pm 0.7 \pm 0.3$	S [2]
$D^+ \to K^+\pi^0$	$0.19 \pm 0.02 \pm 0.01$	$0.0172 \pm 0.0018 \pm 0.0007 \pm 0.0004$	$-3.5 \pm 10.7 \pm 0.9$	S [12]
$D^+ \to K^+\eta$	<0.15 (90% C.L.)	<0.013 (90% C.L.)		N
$D^+ \to \pi^+\eta$	$3.87 \pm 0.09 \pm 0.19$	$0.354 \pm 0.008 \pm 0.018 \pm 0.008$	$-2.0 \pm 2.3 \pm 0.3$	A [20] S [23]
$D^+ \to K^+\eta'$	<0.20 (90% C.L.)	<0.019 (90% C.L.)		N
$D^+ \to \pi^+\eta'$	$5.12 \pm 0.17 \pm 0.25$	$0.468 \pm 0.016 \pm 0.023 \pm 0.010$	$-4.0 \pm 3.4 \pm 0.3$	S [23]
$D_s^+ \to K_S^0 K^+$	100	1.4900 external input	$4.7 \pm 1.8 \pm 0.9$	I [3]
$D_s^+ \to \pi^+\pi^0$	<2.3 (90% C.L.)	<0.037 (90% C.L.)		S [13]
$D_s^+ \to K_S^0\pi^+$	$8.5 \pm 0.7 \pm 0.2$	$0.126 \pm 0.011 \pm 0.003 \pm 0.007$	$16.3 \pm 7.3 \pm 0.3$	S [13]
$D_s^+ \to K^+\pi^0$	$4.2 \pm 1.4 \pm 0.2$	$0.062 \pm 0.022 \pm 0.004 \pm 0.004$	$-26.6 \pm 23.8 \pm 0.9$	S [13]
$D_s^+ \to K^+\eta$	$11.8 \pm 2.2 \pm 0.6$	$0.176 \pm 0.033 \pm 0.009 \pm 0.010$	$9.3 \pm 15.2 \pm 0.9$	S [13]
$D_s^+ \to \pi^+\eta$	$123.6 \pm 4.3 \pm 6.3$	$1.84 \pm 0.06 \pm 0.09 \pm 0.11$	$-4.6 \pm 2.9 \pm 0.3$	S [3]
$D_s^+ \to K^+\eta'$	$11.8 \pm 3.6 \pm 0.7$	$0.18 \pm 0.05 \pm 0.01 \pm 0.01$	$6.0 \pm 18.9 \pm 0.9$	S [13]
$D_s^+ \to \pi^+\eta'$	$265.4 \pm 8.8 \pm 13.9$	$3.95 \pm 0.13 \pm 0.21 \pm 0.23$	$-6.1 \pm 3.0 \pm 0.3$	S [3]

asymmetry errors are $\pm 0.852\%$ for high-momentum kaons (as in 2-body decays), $\pm 0.727\%$ for low-momentum kaons (as in 3-body decays), and $\pm 0.304\%$ for pions.

For D^0 vs $\bar{D}^0$, the only asymmetry we can measure is $K^-\pi^+$ vs $K^+\pi^-$. That difference will contain a component from the difference in the doubly Cabibbo-suppressed decays $D^0 \to K^+\pi^-$ vs $\bar{D}^0 \to K^-\pi^+$, as well as the component from the favored decays $D^0 \to K^-\pi^+$ vs $\bar{D}^0 \to K^+\pi^-$. Our measurement does not separate these two possible asymmetries.

G. Previous CLEO-c measurements

Nearly all of the $D \to PP$ branching fractions reported in this paper have been previously measured by CLEO, using CLEO-c data sets that are subsets of the data samples used here. For D^0 and D^+ decays, typically 281 pb^{-1} from the 818 pb^{-1} data sample was used, and for D_s decays, typically 298 pb^{-1} from the 586 pb^{-1} was used. Some of the earlier measurements detected ηs in the decay mode $\eta \to \pi^+\pi^-\pi^0$ instead of, or in addition to, the $\eta \to \gamma\gamma$ decay mode used here. Thus, four possibilities for superseding earlier results or combining earlier results with measurements in this article can occur:

(i) There was no earlier measurement to be superseded.

(ii) The earlier measurement used a subset of the sample used here, and so the current measurement supersedes the earlier measurement.

(iii) The earlier measurement used $\eta \to \pi^+\pi^-\pi^0$, and so that measurement is statistically independent of the measurement here, and both can be kept, and combined. We consider the systematic errors of the two measurements to be completely correlated.

(iv) The earlier measurement used both $\eta \to \pi^+\pi^-\pi^0$ and $\eta \to \gamma\gamma$. The $\eta \to \gamma\gamma$ component is a subset of the sample used here, and so the earlier result is superseded by this measurement.

In the last column of Table II, we list the references for earlier measurements that are superseded by current measurements or that should be included in averages with current measurements. Only the branching ratios reported here should be used in combination with measurements from elsewhere, since the current measurements are not absolute. Note that not all superseded branching ratios from earlier measurements utilized the normalization mode utilized here.

VI. SUMMARY

The obtained branching ratios, branching fractions, and CP asymmetries for all $D \to PP$ modes are shown in Table II. The values we obtained are consistent with the world averages [16] and for the suppressed modes, of better accuracy. No significant CP asymmetries are observed.

ACKNOWLEDGMENTS

We gratefully acknowledge the effort of the CESR staff in providing us with excellent luminosity and running conditions. D. Cronin-Hennessy thanks the A. P. Sloan Foundation. This work was supported by the National Science Foundation, the U.S. Department of Energy, the Natural Sciences and Engineering Research Council of Canada, and the U.K. Science and Technology Facilities Council.

[1] B. Bhattacharya and J. L. Rosner, Phys. Rev. D **77**, 114020 (2008).
[2] S. Dobbs *et al.* (CLEO Collaboration), Phys. Rev. D **76**, 112001 (2007).
[3] J. P. Alexander *et al.* (CLEO Collaboration), Phys. Rev. Lett. **100**, 161804 (2008).
[4] R. A. Briere *et al.* (CESR-c and CLEO-c Taskforces, CLEO-c Collaboration), Cornell University, LEPP Report No. CLNS 01/1742, 2001 (unpublished).
[5] Y. Kubota *et al.* (CLEO Collaboration), Nucl. Instrum. Methods Phys. Res., Sect. A **320**, 66 (1992).
[6] D. Peterson *et al.*, Nucl. Instrum. Methods Phys. Res., Sect. A **478**, 142 (2002).
[7] M. Artuso *et al.*, Nucl. Instrum. Methods Phys. Res., Sect. A **502**, 91 (2003).
[8] R. Brun *et al.*, GEANT 3.21, CERN Program Library Long Writeup Report No. W5013, 1993 (unpublished).
[9] D. J. Lange, Nucl. Instrum. Methods Phys. Res., Sect. A **462**, 152 (2001).
[10] E. Barberio and Z. Wąs, Comput. Phys. Commun. **79**, 291 (1994).
[11] D. Cronin-Hennessy *et al.* (CLEO Collaboration), Phys. Rev. D **80**, 072001 (2009).
[12] S. A. Dytman *et al.* (CLEO Collaboration), Phys. Rev. D **74**, 071102(R) (2006).
[13] G. S. Adams *et al.* (CLEO Collaboration), Phys. Rev. Lett. **99**, 191805 (2007).
[14] R. M. Baltrusaitis *et al.* (Mark III Collaboration), Phys. Rev. Lett. **56**, 2140 (1986).
[15] J. Adler *et al.* (Mark III Collaboration), Phys. Rev. Lett. **60**, 89 (1988).
[16] C. Amsler *et al.* (Particle Data Group), Phys. Lett. B **667**, 1 (2008).
[17] T. Skwarnicki, Ph.D. thesis, Institute for Nuclear Physics, Krakow, Poland, 1986.
[18] H. Albrecht *et al.* (ARGUS Collaboration), Phys. Lett. B **229**, 304 (1989).
[19] G. Bonvicini *et al.* (CLEO Collaboration), Phys. Rev. D **77**, 091106 (2008).
[20] P. Rubin *et al.* (CLEO Collaboration), Phys. Rev. Lett. **96**, 081802 (2006).
[21] Q. He *et al.* (CLEO Collaboration), Phys. Rev. Lett. **100**, 091801 (2008).
[22] J. L. Rosner *et al.* (CLEO Collaboration), Phys. Rev. Lett. **100**, 221801 (2008).
[23] M. Artuso *et al.* (CLEO Collaboration), Phys. Rev. D **77**, 092003 (2008).